

# Two interacting particles at the metal-insulator transition

Andrzej Eilmes<sup>1</sup>, Uwe Grimm<sup>2</sup>, Rudolf A. Römer<sup>2</sup>, and Michael Schreiber<sup>2</sup>

<sup>1</sup>Department of Computational Methods in Chemistry,

Jagiellonian University, Ingardena 3, 30-060 Kraków, Poland

<sup>2</sup>Institut für Physik, Technische Universität, D-09107 Chemnitz, Germany

(*Revision* : 1.15; compiled October 16, 2018)

## Abstract

To investigate the influence of electronic interaction on the metal-insulator transition (MIT), we consider the Aubry-André (or Harper) model which describes a quasiperiodic one-dimensional quantum system of non-interacting electrons and exhibits an MIT. For a two-particle system, we study the effect of a Hubbard interaction on the transition by means of the transfer-matrix method and finite-size scaling. In agreement with previous studies we find that the interaction localizes some states in the otherwise metallic phase of the system. Nevertheless, the MIT remains unaffected by the interaction. For a long-range interaction, many more states become localized for sufficiently large interaction strength and the MIT appears to shift towards smaller quasiperiodic potential strength.

71.30.+h, 71.27.+a, 72.15.Rn, 71.23.Ft

## I. INTRODUCTION

The physics of the metal-insulator transition (MIT) continues to be at the center of current research activities. For two decades it has been known from the scaling hypothesis of localization [1] that generically a disorder-driven MIT [2] in a free electron system only occurs in more than two spatial dimensions, whereas in one or two dimensions an arbitrarily small disorder will localize the electronic wave functions. The relevance of many-particle interactions for the MIT is much less understood [3,4]. Here we consider the perhaps simplest tractable model of an interacting system at the MIT. Namely, we study the case of just two interacting particles (TIP) in a particular one-dimensional (1D) quasiperiodic (QP) potential. For a single particle (SP) this QP model exhibits an MIT as a function of the non-random QP potential strength.

The problem of TIP in a 1D random potential, where the wave functions are always localized such that there is no MIT, has already been studied in much detail [5–13]. It was argued that a Hubbard onsite interaction  $U$  dramatically reduces the localization of TIP pair states in comparison with non-interacting and unpaired particles. In particular, Shepelyansky [5,6] proposed an enhancement of the TIP localization length  $\lambda_2$  independent of the statistics of the particles and of the sign of the interaction such that

$$\lambda_2(U) \approx U^2 \frac{\lambda_1^\kappa}{32} \quad (1)$$

in the band center with  $\kappa = 2$ . Here,  $\lambda_1$  is the SP localization length in 1D [14] and  $U$  is given in units of the nearest-neighbor hopping strength. Microscopic support for the delocalization was given afterwards by Frahm *et al.* [8], who observed a behavior  $\lambda_2 \sim \lambda_1^{1.65}$  in a numerical investigation employing the transfer-matrix method (TMM). Other direct numerical approaches to the TIP problem have been based on the time evolution of wave packets [5,15], exact diagonalization [10], Green function approaches [9,12,16], and TMM [11,17]. In these investigations an enhancement of  $\lambda_2$  compared to  $\lambda_1$  has usually been found, but the quantitative results tend to differ both from the analytical prediction (1), and from each other.

Two of us [11] recently studied the TIP problem by TMM but at larger system sizes  $M$  than Ref. [8] and found that (i) the enhancement  $\lambda_2/\lambda_1$  decreases with increasing  $M$ , (ii) the behavior of  $\lambda_2$  for  $U = 0$  is equal to  $\lambda_1$  in the limit  $M \rightarrow \infty$  only, and (iii) for  $U \neq 0$  the enhancement  $\lambda_2/\lambda_1$  also vanishes completely in this limit. This raises serious questions about the validity of the TMM approach to TIP and in fact it has been argued very recently [18], that the TMM approach of Ref. [8,11] may systematically underestimate the localization length of a pair state, since it automatically measures a mixture of localization lengths originating also from unpaired states. Thus in this work, we will use the TIP-TMM not as a tool to extract information about the pair states only, but rather aim at describing the general influence of the presence of one particle onto the transport properties of the other.

At present, it seems well-established by Green function methods [9,12,16] that an enhancement  $\lambda_2 > \lambda_1$  exists, although the validity of Eq. (1) is still under debate: the values of the exponent  $\kappa$  obtained by numerical methods [5,8–12,15–17] range from 1 to 2. In spite of these numerical differences, we nevertheless believe that the TIP approach can give meaningful insights into the interplay of disorder and interaction [16]. In particular, the effects of interaction on the disorder-driven Anderson transition should be quite interesting already for TIP. However, as mentioned above, the disorder-driven MIT requires more than two spatial dimensions and so the numerical efforts are close to being prohibitive when including interactions.

Fortunately, the QP — and thus fully deterministic — Aubry-André (AA) model [19] exhibits an MIT even in 1D, in dependence on the strength of the quasiperiodic potential. This model is closely related to the problem of a SP on a 2D lattice in a magnetic field in which context it is also known as the Harper model [20]. At the MIT, the spectrum exhibits the famous Hofstadter butterfly shape [21], and the spectral and localization properties have been studied in great detail [22]. In the mathematical literature, the same model is also known and studied as the almost-Mathieu equation [23].

For this 1D model, we can use the TIP approach in a straightforward way in order to investigate the effect of the interaction on the transition. Previous studies based on

perturbative expansions in  $U$  and numerical computations of participation numbers in the AA model [24] concluded that interaction can lead to the appearance of localized states in the metallic regime for TIP. However, although participation numbers are a useful tool for characterizing localization properties of states, they may give ambiguous results: in some cases, states which are extended or critical may appear to be more localized and vice versa [25]. Moreover, for interacting particles the generalization of localization criteria like the participation number is not straightforward [26]. Thus in this work we concentrate on direct calculations of the TIP localization length in the AA model using the TMM for finite system sizes. In addition to the onsite interaction, we also consider a long-range interaction. Employing the finite-size-scaling (FSS) approach [27], we then construct scaling curves from which we deduce the localization properties of the infinite system. We find that within the accuracy of our results, the critical behavior is not affected by the interactions. But it seems that the long-range interaction shifts the critical QP potential strengths towards smaller values, thus giving a tendency towards localization.

The paper is organized as follows. In section II, we define the TIP version of the AA model and introduce our notations. Section III reviews the power-series variant of the TMM, and the concepts of FSS. In section IV we explain the use of a phase-shift parameter in the QP potential for reducing statistical fluctuations in the localization length data. Results obtained from FSS of the localization lengths for Hubbard and long-range interactions at energy  $E = 0$  are presented in section V. In section VI, we show the localization properties of all states of the spectrum. We summarize and conclude in section VII.

## II. THE TIP VERSION OF THE AUBRY-ANDRÉ MODEL

The Schrödinger equation for the SP AA model is given as

$$\phi_{n+1} = (E - \mu_n)\phi_n - \phi_{n-1}. \quad (2)$$

Here  $\phi_n$  is a SP wave function,  $\mu_n \equiv 2\mu \cos(\alpha n + \beta)$  is the QP AA onsite potential of strength  $\mu$  with  $\alpha/2\pi$  an irrational number, which we have chosen as the inverse of the golden mean

$\alpha/2\pi = (\sqrt{5} - 1)/2$ , and  $\beta$  is an arbitrary phase shift. We remark that  $\alpha/2\pi$  may be approximated by the ratio of successive Fibonacci numbers 1, 2, 3, 5, 8, 13,  $\dots$ . In Fig. 1 we show typical data for the SP localization length  $\lambda_1$  obtained by TMM for various system sizes given by some of the Fibonacci numbers [28]. In agreement with previous studies [19], this figure suggests already that the MIT occurs at  $\mu = 1$ . Of course, further analysis like FSS would be necessary for a comprehensive study of this MIT. Here we note that in contradistinction to the MIT in the usual Anderson model with onsite *random* potential disorder, in the AA model *all* states are either extended ( $\mu < 1$ ), critical ( $\mu = 1$ ), or localized ( $\mu > 1$ ), and thus no mobility edge, i.e., no MIT in dependence *on energy* exists.

In principle, there are many possibilities to extend the SP Schrödinger equation to TIP. In order to be most compatible with the TIP approach of Shepelyansky [5], we will consider a TIP Hamiltonian with an additional QP onsite potential on a chain of length  $M$  given as

$$\begin{aligned}
H = & \sum_{n=1}^M (c_{n+1}^\dagger c_n + h.c.) + \sum_{n=1}^M \sum_{m=1}^M U_{n,m} c_n^\dagger c_n c_m^\dagger c_m, \\
& + \sum_{n=1}^M \mu_n c_n^\dagger c_n
\end{aligned} \tag{3}$$

where  $c_n^\dagger$  and  $c_n$  are the creation and annihilation operators for the electron at site  $n$  and we assume that the TIP have different spins.  $U_{n,m}$  denotes the interaction between particles:  $U_{n,m} = U\delta_{nm}$  for Hubbard onsite interaction or  $U_{n,m} = U/(|n - m| + 1)$  for long-range interaction.

### III. THE TRANSFER-MATRIX APPROACH TO TIP

The TIP Schrödinger equation reads

$$\begin{aligned}
\psi_{n+1,m} = & [E - U_{n,m} - \mu_n - \mu_m] \psi_{nm} \\
& - \psi_{n,m+1} - \psi_{n,m-1} - \psi_{n-1,m},
\end{aligned} \tag{4}$$

with  $\psi_{n,m}$  a TIP wave function which at  $U = 0$  may be written as a product of SP wave functions  $\phi_n$  and  $\phi_m$ . We can rewrite Eq. (4) in the TMM form similar to a 2D Anderson

model on an  $M \times M$  lattice as  $(\psi_{n+1}, \psi_n)^T = T_n(\psi_n, \psi_{n-1})^T$  with the symplectic transfer matrix

$$T_n = \begin{pmatrix} E\mathbb{1} - \chi_n - H_\perp & -\mathbb{1} \\ \mathbb{1} & \mathbf{0} \end{pmatrix}, \quad (5)$$

describing the evolution of the wave vectors for the first ( $n$ ) particle (corresponding to the longitudinal direction in the 2D SP TMM approach). Here  $\psi_n = (\psi_{n,1}, \dots, \psi_{n,m}, \dots, \psi_{n,M})$  is the wave vector of slice  $n$ ,  $H_\perp$  is the SP hopping term for the second ( $m$ ) particle (corresponding to the transverse direction) and  $(\chi_n)_{i,m} = [\mu_n + \mu_m + U_{n,m}]\delta_{i,m}$  codes the QP potential and the interaction [8]. Note that in this approach the symmetry of the wave function remains unspecified and we cannot distinguish between boson and fermion statistics.

The evolution of the state is determined by the matrix product  $\tau_N = \prod_{n=1}^N T_n$  and we have

$$\begin{pmatrix} \psi_{N+1} \\ \psi_N \end{pmatrix} = \tau_N \begin{pmatrix} \psi_1 \\ \psi_0 \end{pmatrix}. \quad (6)$$

Usually, one studies a quasi-1D system of size  $M \times N$  with  $M \ll N$ . However, in the present problem, both directions are restricted to  $n, m \leq M$  and iterating Eq. (6) only  $N = M$  times will not give convergence. Frahm *et al.* [8] have solved this problem in their TMM study by exploiting the Hermiticity of the product matrix  $Q_M = \tau_M^\dagger \tau_M$ : Continuing the iteration (6) with  $\tau_M^\dagger$ , then with  $\tau_M$ , and so on, until convergence is achieved, yields the eigenvalues  $\exp[-2M\gamma_i]$  of  $Q_M$ . This is the well-known power method for the diagonalization of Hermitian matrices [29]. The smallest positive Lyapunov exponent  $\gamma_{\min}$  determines the slowest possible decay of the wave function and thus the largest localization length  $\lambda_{\max} = 1/\gamma_{\min}$  for given energy  $E$  and phase shift  $\beta$ . We now *define* the localization length  $\lambda$  of the two-particle wave function  $\psi_{n,m}$  as  $\lambda_{\max}$  of the transfer matrix problem (6) and expect it to reflect the influence of the particle interaction.

According to the one-parameter scaling hypothesis [1], which has been verified with very high accuracy for random potentials  $\mu_n$  [27], the reduced localization lengths  $\lambda(M)/M$  scale onto a single scaling curve, i.e.,

$$\lambda(M)/M = f(\xi/M). \quad (7)$$

For the AA model considered here, we are not aware of any previous FSS study. Indeed, it is not a priori obvious that one-parameter FSS should be valid for the AA model. At least for a given single phase shift  $\beta$ , it is clear from Fig. 1 that we need to go to rather large system sizes in order to suppress the fluctuations around  $\mu = 1$  and to be able to use the FSS approach. However, as we will explain in the next section, we may use different values of  $\beta$  as being analogous to the different disorder realizations in the Anderson model. As usual, we may then determine the finite-size-scaling (FSS) function  $f$  and the values of the scaling parameter  $\xi$  by a least-squares fit [27].

#### IV. AVERAGING OVER DIFFERENT $\beta$

The localization length calculated for given system size and QP potential  $\mu$  depends significantly on the  $\beta$  value as shown for SP in Fig. 2. This means that the decay length varies depending on the phase shift of the potential along the chain. One may expect that the chain length  $M$  will also influence the results by changing relative phases of the potential at the ends.

Therefore we have restricted our calculations to the chain lengths given by the Fibonacci numbers mentioned in section II, because for our choice of  $\alpha$ , this assures that the phase difference of the potential at both ends of the chain will be similar, i.e., approaching zero with increasing  $M$ . We note that our numerical results presented in the next section do not change significantly, when we alternatively use the rational approximants for  $\alpha/2\pi$  instead of the irrational number defined in section II.

Still, the dependence of  $\lambda_1$  on the system size  $M$  for a given value of  $\beta$  shows much structure which makes simple extrapolations towards the infinite system or FSS impossible. This dependence is also responsible for fluctuations of the SP  $\lambda_1$  close to  $\mu = 1$  which are visible as peaks in Fig. 1 for small Fibonacci number  $M$  [28]. Only for very large  $M$ , the fluctuations become small. On the other hand, finite systems with different values of  $\beta$  may

be viewed as different parts cut out of the infinite QP model. This then suggests that we may reduce the fluctuation effects by averaging over many such small pieces or, equivalently, many different values of randomly chosen  $\beta$ . Thus different  $\beta$  values are analogous to different disorder configurations used in the Anderson Hamiltonian. Fig. 3 presents such an average over 1000  $\beta$  values for the SP localization length. As expected, the fluctuations visible in Fig. 1 disappear even for small systems and extrapolations to large  $M$  and FSS are now possible.

## V. LOCALIZATION PROPERTIES AT $E = 0$

We now turn our attention to the problem of TIP and study the effects of interaction on the localization lengths obtained by TMM, restricting ourselves to  $E = 0$ . To this end, we have computed the localization lengths for 6 system sizes  $M = 8, 13, 21, 34, 55,$  and  $89$ , for 80 QP potential strengths  $\mu$  ranging from 0.56 to 4, and for 6 interaction strengths  $U = 0, 0.5, 1, 1.5, 2,$  and  $10$ , with onsite and with long-range interaction. Typically, for each such triplet of parameters  $(M, \mu, U)$  we averaged over at least 1000 different  $\beta$  realizations. We note that as for the case of TIP in a random potential [16], attractive and repulsive interaction strengths give the same results at  $E = 0$  and we can thus restrict ourselves to  $U \geq 0$  here.

### A. Hubbard interaction

Figs. 4 and 5 show the FSS results for  $\beta$ -averaged data at energy  $E = 0$  for onsite interaction strength  $U = 0$  and  $U = 1$ . As can be seen, the coalescence of data for various values of  $\mu$  is not perfect and in fact certainly worse than, e.g., for onsite random disorder [27]. This is especially visible on the extended side  $\mu < 1$ . Nevertheless, the figures clearly show the existence of two branches of the scaling curve as in the 3D Anderson model [27]. This indicates, in agreement with the above considerations for the SP AA model, the presence of localized states for  $\mu > 1$  and extended states for  $\mu < 1$ . The MIT appears at a critical



QP potential  $\mu_c$  which is close to 1. The values determined from the FSS procedure are  $\mu_c = 1.01 \pm 0.02$  for  $U = 0$  and  $\mu_c = 1.04 \pm 0.04$  for  $U = 1$ . Corresponding FSS plots for  $U = 0.5, 1.5, 2$  and  $10$  all consistently give  $\mu_c \approx 1$ . We attribute the small deviations from the critical value  $\mu_c = 1$  of the SP case to the fluctuations in the data.

Thus the MIT does not get shifted by the Hubbard interaction and the transport properties of one particle in the presence of another remain unchanged. On the metallic side of the transition ( $\mu < 1$ ) this is immediately clear: the interaction is supposed to localize  $\mathcal{O}(M)$  TIP states out of the  $\mathcal{O}(M^2)$  states in the unsymmetrized Hilbert space [24]. The TMM inherently measures the longest localization length and thus simply misses the few shorter localization lengths induced by the interaction. On the localized side, however, we could expect the interaction to delocalize these TIP states which might be visible even by TMM. However, as discussed in section I, this effect is not present in the TIP-TMM or at least too small to be visible [18].

The scaling parameters  $\xi$  obtained by FSS according to Eq. (7) are expected to diverge at the transition as  $\xi \sim |\mu - \mu_c|^{-\nu}$  with the critical exponent  $\nu$ . In Fig. 6 we show the dependence of  $\xi$  on the QP strength  $\mu$ . The divergence at  $\mu_c \approx 1$  is clearly visible. A power-law fit gives  $\nu = 0.8 \pm 0.2$  both for  $U = 0$  and  $U = 1$ . The large error of the estimate is due to the fluctuations in the data near the critical point [27]. Furthermore, in the localized regime of the SP AA model it has been shown that [19]

$$\lambda_1 \sim 1/\ln(1 + |\mu - \mu_c|), \quad (8)$$

which yields  $\nu = 1$  by expansion around  $\mu_c$ . In order to check whether this equation holds also for TIP we examined the dependence of  $1/\xi$  on  $\ln(1 + |\mu - \mu_c|)$ . The results are displayed in Fig. 7. The slope of the best fit line is  $1.00 \pm 0.02$  for  $U = 0$  and  $1.01 \pm 0.03$  for  $U = 1$ . This suggests that onsite interaction does not change the critical behavior at the MIT.

## B. Long-range interaction

We now consider the long-range interaction defined in section II. The FSS plot for  $U = 1$  in Fig. 8 is qualitatively the same as for Hubbard interaction. We find localized states for  $\mu \gg 1$  and extended states for  $\mu \ll 1$ . In Fig. 6, we have included the variation of the scaling parameter  $\xi$  with  $\mu$  for this case. The divergence of  $\xi$  occurs at  $\mu_c = 0.92 \pm 0.04$  indicating that the MIT has been shifted towards smaller values of the QP potential strength  $\mu$ . FSS plots for  $U = 0.5, 1.5$  and  $2$  suggest that this shift becomes somewhat more pronounced for larger  $U$ , decreasing to  $\mu_c \approx 0.9$  for  $U = 2$ .

This behavior may be rationalized by keeping in mind that for a long-range interaction, contrary to the case of Hubbard interaction, *all* states will eventually feel the interaction-induced tendency towards localization on the extended side of the MIT, as we will show for small systems in the next section. Thus even the most delocalized states at  $E = 0$  will become more localized for sufficiently large  $U$ . However, in order to answer the question whether long-range interaction indeed shifts the MIT towards weaker QP potential strength, additional calculations with still higher accuracy would be necessary. These require, however, a prohibitive numerical effort when using the present power-series method.

The critical exponent for  $U = 1$  calculated as in section V A is  $\nu = 1.0 \pm 0.2$  and the respective slope in Fig. 7 is  $0.97 \pm 0.03$ . These values are compatible with our results for onsite interaction within the error limits. Therefore, the critical behavior is similar to the SP case and onsite interaction.

## VI. ENERGY DEPENDENCE OF THE LOCALIZATION PROPERTIES

In the previous section, we have rationalized the persistence of the MIT in the presence of interactions by assuming that on the extended side the onsite interaction localizes a small number of states leaving the rest unaffected. To further examine this effect with TMM we calculate the dependence of  $\lambda$  on the energy  $E$  for a single value of  $\beta$  and a small system

size.

### A. Hubbard interaction

Fig. 9 presents results for the inverse localization length  $\lambda^{-1}$  obtained by TMM on the metallic side. Also shown are the values of the eigenenergies  $E_i$ . The TMM accurately shows that transport at energies not corresponding to eigenstates is suppressed, because the incoming wave function decays exponentially. On the other hand,  $\lambda^{-1}(E)$  decreases rapidly towards zero when  $E$  is approaching an eigenvalue  $E_i$  as shown in Fig. 9. This has also been observed in the SP case [19]. For  $U = 0$ , we find a few cases where  $\lambda^{-1}$  remains large even at the energy of an eigenstate. From an analysis of the corresponding wave functions, we can identify these states with boundary states where the particles are localized close to the ends of the finite chains.

The comparison of the plots for  $U = 0$  and  $U = 1$  shows that, while the energy of most states changes only slightly, there are a few states which move to significantly larger energies. Their localization lengths are apparently much shorter. The calculation of  $\beta$ -averaged decay lengths for different  $M$  shows that states at the verge of the spectrum at  $E = 4.6$  remain extended for  $U = 1$  while the states at  $E = 5.3$  are localized. There are also some states within the main part of the spectrum which shift to higher energies. Some of them are visible in Fig. 9 as they enter the energy gaps. For sufficiently strong interaction  $U = 8$  there are 13 localized states which split off the remaining spectrum. The calculations for other system sizes support the conclusion that the interaction localizes  $M$  out of  $M^2$  states for system size  $M$ . These states correspond to both particles residing on the same site and interacting via the Hubbard  $U$ . The other states remain extended and do not change their energy significantly.

In the localized regime ( $\mu > 1$ ) the interaction has a similar effect, i.e., for sufficiently large  $U$  it shifts  $M$  states above the main part of the spectrum and increases their localization; the remaining unshifted states also stay localized. These results are in agreement with

those of Ref. [24], when we keep in mind that our numerical method does not allow us to see accurately an eventual delocalization at intermediate  $U$ .

### B. Long-range interaction

Fig. 10 presents respective results obtained for long-range interaction. Again, the interaction shifts states to higher energies and shortens their decay lengths. However, as the particles feel the interaction at any separation, *all* states change their energy in agreement with section V B. This is especially pronounced in Fig. 10 for  $U = 10$ . The most prominent shift is the change at the high energy part of the spectrum. For extremely large interaction, e.g.  $U = 1000$ , the spectrum splits into  $M$  groups of states reflecting the number of sites at which two particles may reside at given separation, i.e., for system size  $M$  there are  $M$  states for separation  $n - m = 0$ , and  $2M - 2$  states for separation  $|n - m| = 1$ , and so on.

## VII. CONCLUSIONS

We have demonstrated that it is possible to perform FSS for a system with two interacting particles in a 1D QP Aubry-André (or Harper) potential. We find two branches in the FSS curves which correspond to localized and extended behavior. The roughness of the FSS plot is probably an effect of small system sizes and insufficient averaging and should disappear for larger systems, requiring, however, much larger computational effort. On the other hand it may be that one-parameter scaling is not strictly valid in this QP model as evidenced by the results for the even chain lengths  $M = 34$  and  $144$  [28]. Nevertheless, even in this case the presence of localized and extended branches as in Figs. 4, 5, 8 indicates the existence of an MIT.

The FSS results for energy  $E = 0$  show that the MIT exists in these TIP systems both for the non-interacting and the interacting case. The transition point  $\mu_c$  does not depend on the Hubbard interaction strength  $U$  and is located at QP potential strength  $\mu_c \approx 1$ . However, a large enough long-range interaction shifts  $\mu_c$  towards smaller QP strength. Within the

numerical accuracy of our data, the critical behaviour of the localization length is not affected by the Hubbard and the long-range interaction.

The dependence of the decay length on the energy as calculated by TMM confirms the results obtained by other methods [19] that a large enough interaction localizes pair states simultaneously increasing their energy and leaves the rest of the states almost unaffected.

In closing we remark that our results may also be viewed independently of the TIP problem, by noting that the present problem of two particles in a 1D QP potential may also be seen as SP problem in a particular realization of a 2D QP potential. Similar systems have been investigated previously, e.g., in Ref. [30] within the Landauer approach.

#### ACKNOWLEDGMENTS

We thank K. Frahm and J.-L. Pichard for a clarifying discussion on the power series method. A.E. expresses his gratitude to the Foundation for Polish Science for a fellowship. This work has been supported by the Deutsche Forschungsgemeinschaft (SFB 393).

## REFERENCES

- [1] E. Abrahams, P. W. Anderson, D. C. Licciardello, and T. V. Ramakrishnan, Phys. Rev. Lett. **42**, 673 (1979).
- [2] P. W. Anderson, Phys. Rev. **109**, 1492 (1958).
- [3] D. Belitz and T. R. Kirkpatrick, Rev. Mod. Phys. **66**, 261 (1994).
- [4] S. V. Kravchenko, D. Simonian, and M. P. Sarachik, Phys. Rev. Lett. **77**, 4938 (1996); V. M. Pudalov, G. Brunthaler, A. Prinz, and G. Bauer, preprint (1997, cond-mat/9707054); B. L. Altshuler and D. L. Maslov, preprint (1998, cond-mat/9807245); and references therein.
- [5] D. L. Shepelyansky, Phys. Rev. Lett. **73**, 2607 (1994).
- [6] D. L. Shepelyansky, in *Correlated fermions and transport in mesoscopic systems*, Eds. T. Martin, G. Montambaux, and J. Trân Thanh Vân, Editions Frontieres, Gif-sur-Yvette, p. 201 (1996) (Proc. XXXI Moriond Workshop, 1996).
- [7] Y. Imry, Europhys. Lett. **30**, 405 (1995).
- [8] K. Frahm, A. Müller-Groeling, J. L. Pichard, and D. Weinmann, Europhys. Lett. **31**, 169 (1995).
- [9] F. v. Oppen, T. Wettig, and J. Müller, Phys. Rev. Lett. **76**, 491 (1996).
- [10] D. Weinmann, A. Müller-Groeling, J.-L. Pichard, and K. Frahm, Phys. Rev. Lett. **75**, 1598 (1995); T. Vojta, R. A. Römer, and M. Schreiber, preprint (1997, cond-mat/9702241).
- [11] R. A. Römer and M. Schreiber, Phys. Rev. Lett. **78**, 515 (1997); K. Frahm, A. Müller-Groeling, J.-L. Pichard, and D. Weinmann, Phys. Rev. Lett. **78**, 4889 (1997); R. A. Römer and M. Schreiber, Phys. Rev. Lett. **78**, 4890 (1997).
- [12] P. H. Song and D. Kim, Phys. Rev. B **56**, 12217 (1997).

- [13] I. V. Ponomarev and P. G. Silvestrov, *Phys. Rev. B* **56**, 3742 (1997).
- [14] G. Czycholl, B. Kramer, and A. MacKinnon, *Z. Phys. B* **43**, 5 (1981); J.-L. Pichard, *J. Phys. C* **19**, 1519 (1986).
- [15] D. Brinkmann, J. E. Golub, S. W. Koch, P. Thomas, K. Maschke, and I. Varga, preprint (1998).
- [16] M. Leadbeater, R. A. Römer, and M. Schreiber, preprint (1998, cond-mat/9806255); —, preprint (1998, cond-mat/9806350).
- [17] O. Halfpap, A. MacKinnon, and B. Kramer, to be published in *Sol. State Comm.*, (1998); O. Halfpap, I. Kh. Zharekeshev, B. Kramer, and A. MacKinnon, preprint (1998).
- [18] P. H. Song and F. v. Oppen, preprint (1998, cond-mat/9806303); K. Frahm, private communication.
- [19] S. Aubry and G. André, *Ann. Israel Phys. Soc.* **3**, 133 (1980).
- [20] P. G. Harper, *Proc. Phys. Soc. London Sect. A* **68**, 874 (1955).
- [21] D. R. Hofstadter, *Phys. Rev. B* **14**, 2239 (1976).
- [22] M. Kohmoto, *Phys. Rev. Lett.* **51**, 1198 (1983); M. Kohmoto, L. P. Kadanoff, and C. Tang, *Phys. Rev. Lett.* **50**, 1870 (1983); S. Ostlund, R. Pandit, D. Rand, H. J. Schellnhuber, and E. D. Siggia, *Phys. Rev. Lett.* **50**, 1873 (1983); S. Ostlund and R. Pandit, *Phys. Rev. B* **29**, 1394 (1984); S. Das Sarma, S. He, and X. C. Xie, *Phys. Rev. B* **41**, 5544 (1990); I. Varga, J. Pipek, and B. Vasvári, *Phys. Rev. B* **46**, 4978 (1992).
- [23] J. Bellissard, R. Lima, and D. Testard, *Commun. Math. Phys.* **88**, 207 (1983); B. Simon, *Adv. Appl. Math.* **3**, 463 (1982).
- [24] A. Borelli, J. Bellissard, P. Jacquod, and D. L. Shepelyansky, *Phys. Rev. Lett* **77**, 4752 (1996), *Phys. Rev. B* **55**, 9524 (1997); D. L. Shepelyansky, *Phys. Rev. B* **54**, 14896 (1996).

- [25] A. Eilmes, R. A. Römer, and M. Schreiber, *Eur. Phys. J. B* **1**, 29 (1998).
- [26] T. Vojta, F. Epperlein, and M. Schreiber, *phys. stat. sol. (b)* **205**, 53 (1998).
- [27] A. MacKinnon and B. Kramer, *Z. Phys. B* **53**, 1 (1983).
- [28] For  $M$  an even Fibonacci number, we find that the SP localization lengths on the extended side  $\mu < 1$  show a qualitatively different behavior, shifting towards much larger localization lengths. This may be related to the fact that the QP potential  $\mu_n \approx -\mu_{n+M/2}$  for all  $n = 1, \dots, M/2$ . For TIP this shift is much less pronounced.
- [29] R. A. Horn and C. R. Johnson, *Matrix Analysis*, Cambridge University Press, New York (1985).
- [30] U. Grimm, F. Gagel, and M. Schreiber, in *Quasicrystals: Proceedings of the 6th Int. Conference*, eds. S. Takeuchi and T. Fujiwara, p. 188 (World Scientific, Singapore, 1998).



FIGURES

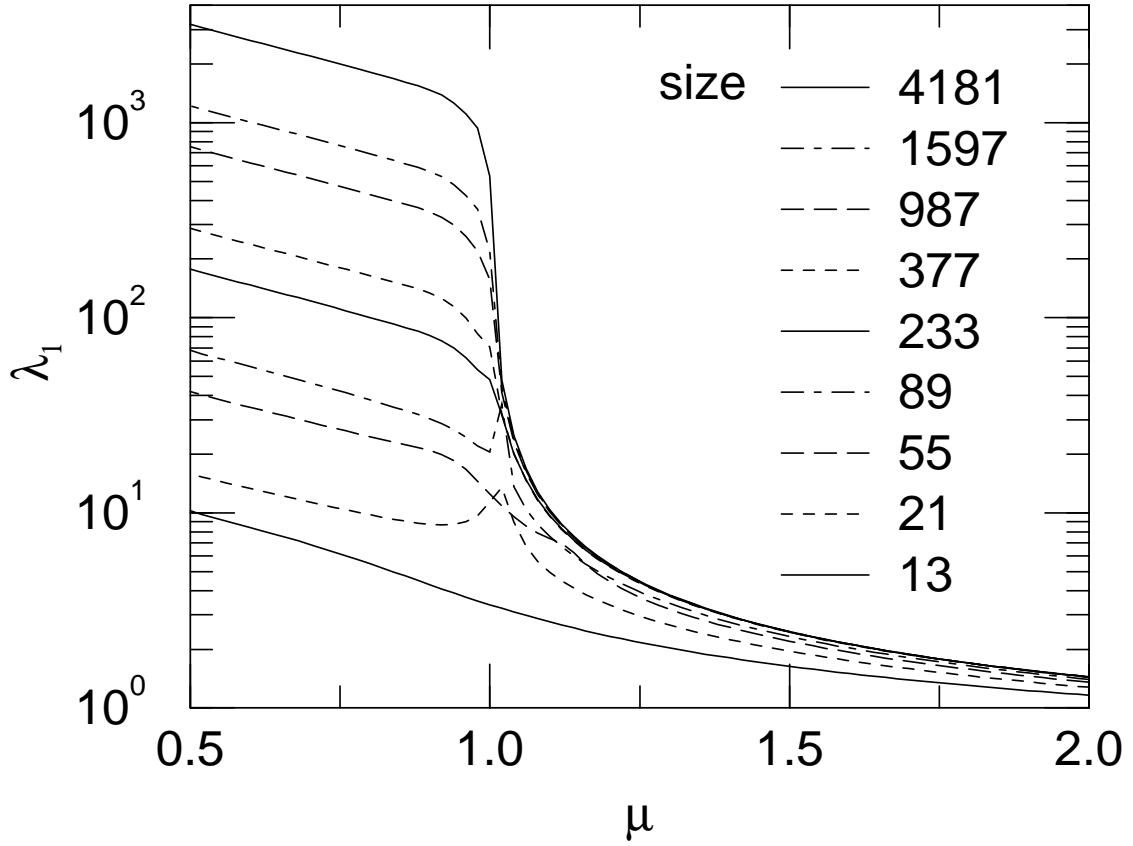


FIG. 1. Localization length  $\lambda_1$  for the SP Aubry-André model as a function of QP potential strength  $\mu$  for  $E = 0$  and  $\beta = \sqrt{2}$  with system size increasing from bottom to top.

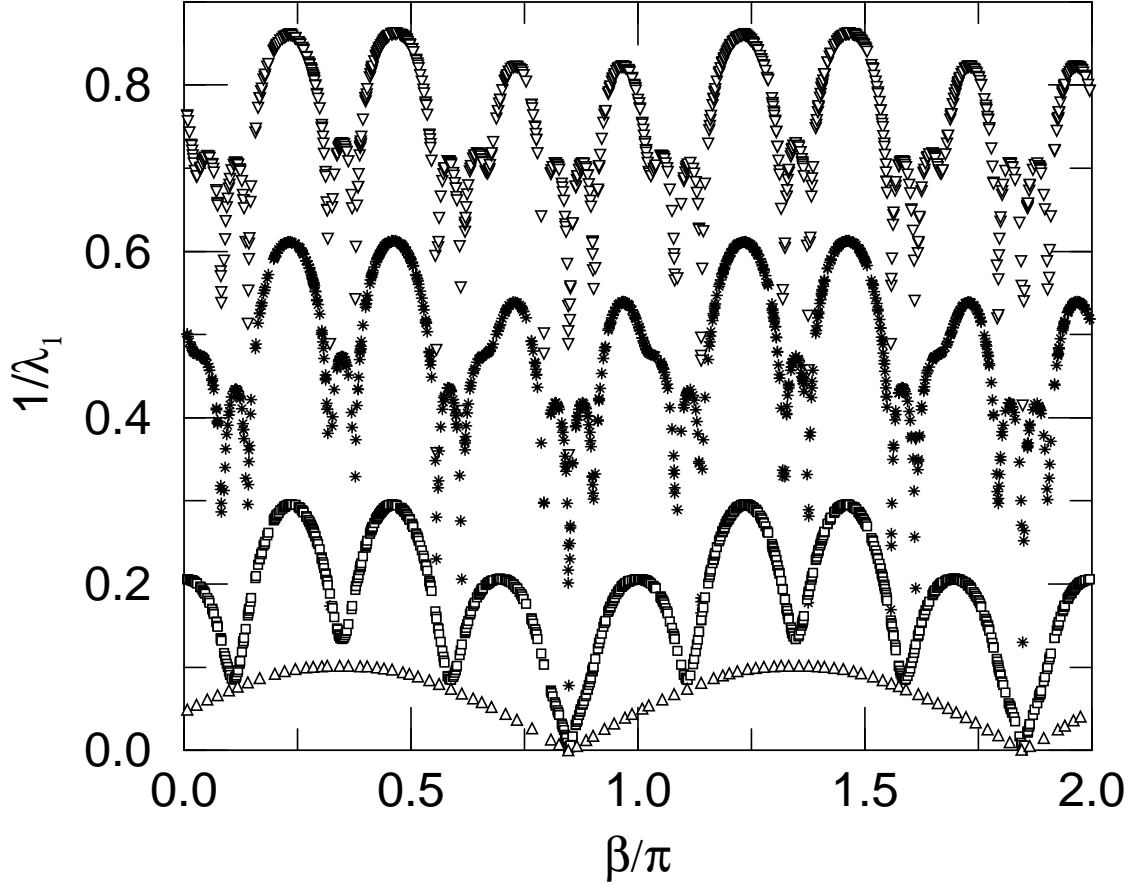


FIG. 2. Inverse of the localization length  $\lambda_1$  for the SP Aubry-André model as a function of phase shift  $\beta$  for  $E = 0$  and  $M = 13$ . Different symbols indicate QP potential strength  $\mu = 2$  ( $\nabla$ ), 1.5 ( $*$ ), 1 ( $\square$ ), and 0.5 ( $\triangle$ ).

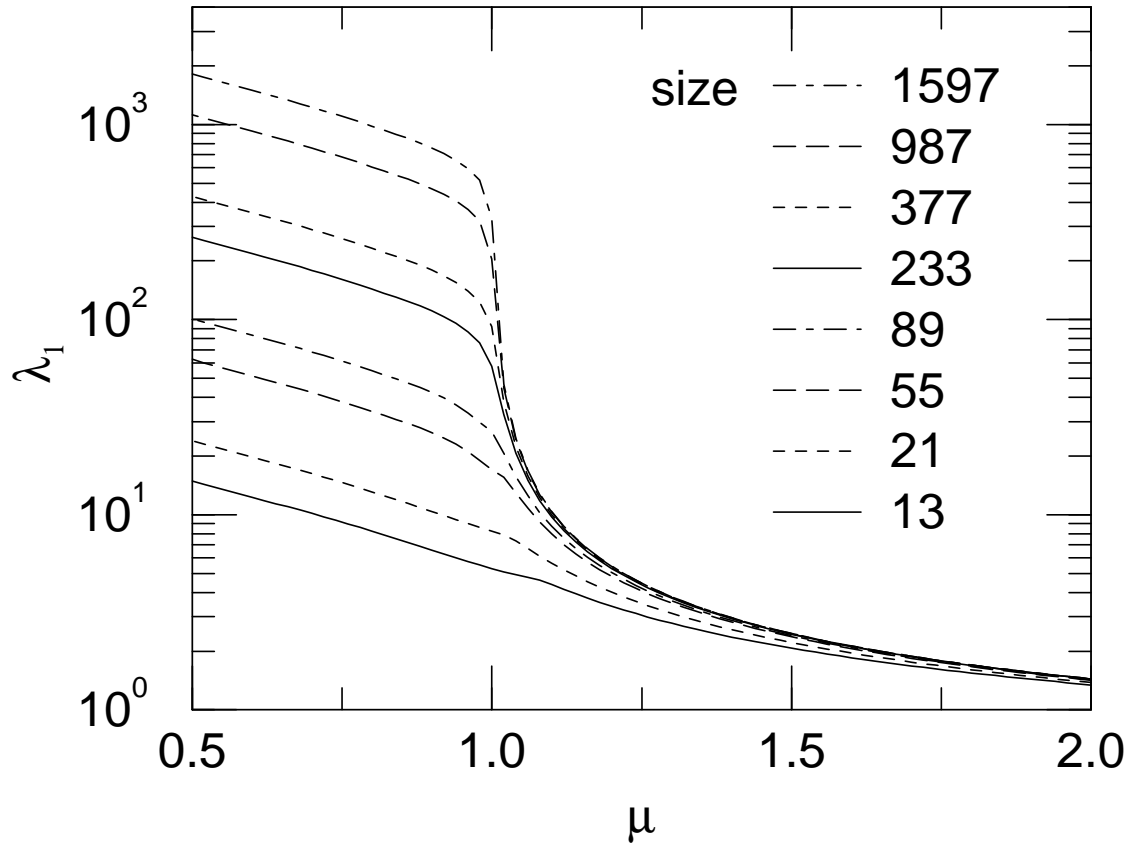


FIG. 3. Localization length  $\lambda_1$  for the SP Aubry-André model as a function of QP potential strength  $\mu$  for  $E = 0$ , averaged over 1000  $\beta$ -values. The system size is increasing from bottom to top. Note the MIT at  $\mu = 1$ .

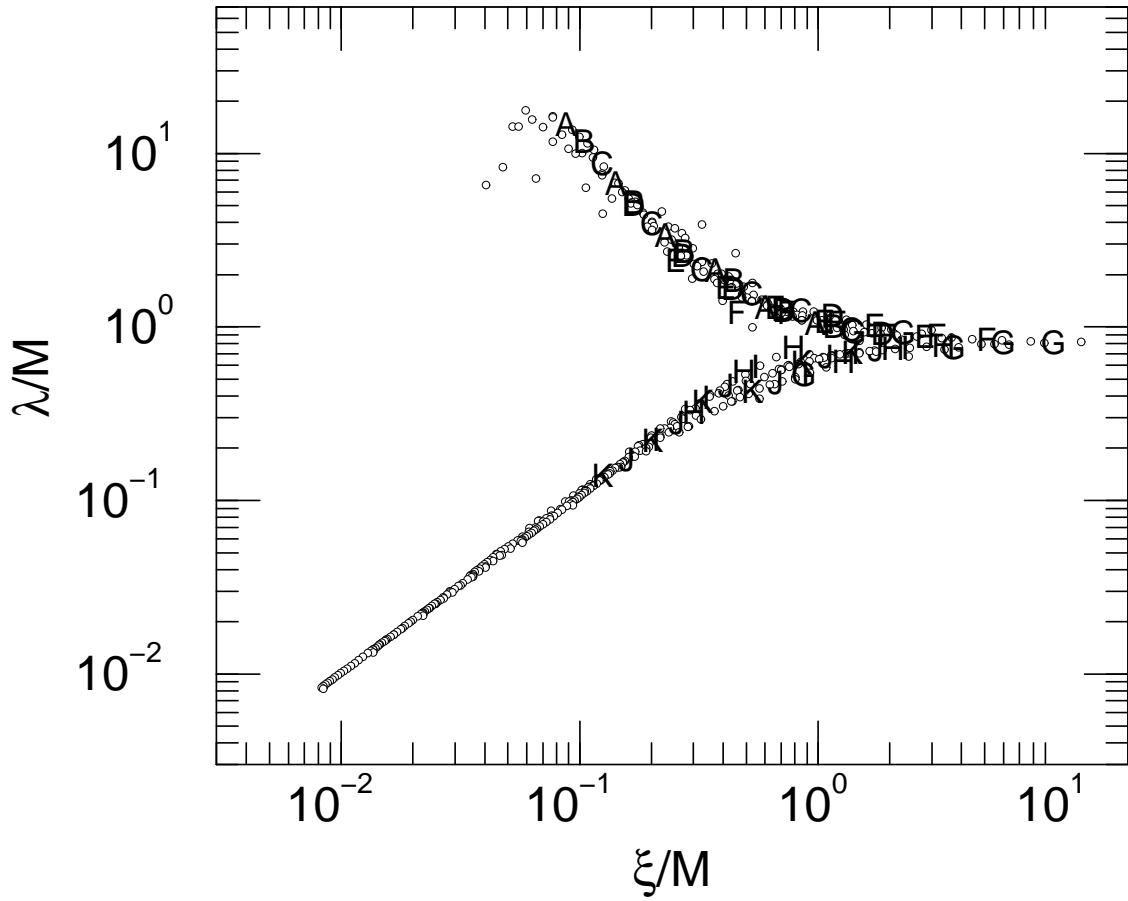


FIG. 4. Scaling function (7) for  $U = 0$ ,  $E = 0$  and various  $\mu$ . Data for  $\mu = 0.9, 0.92, 0.94, 0.96, 0.98, 1.0, 1.02, 1.04, 1.06, 1.08$ , and  $1.1$  are marked with characters A, B,  $\dots$ , K, respectively.

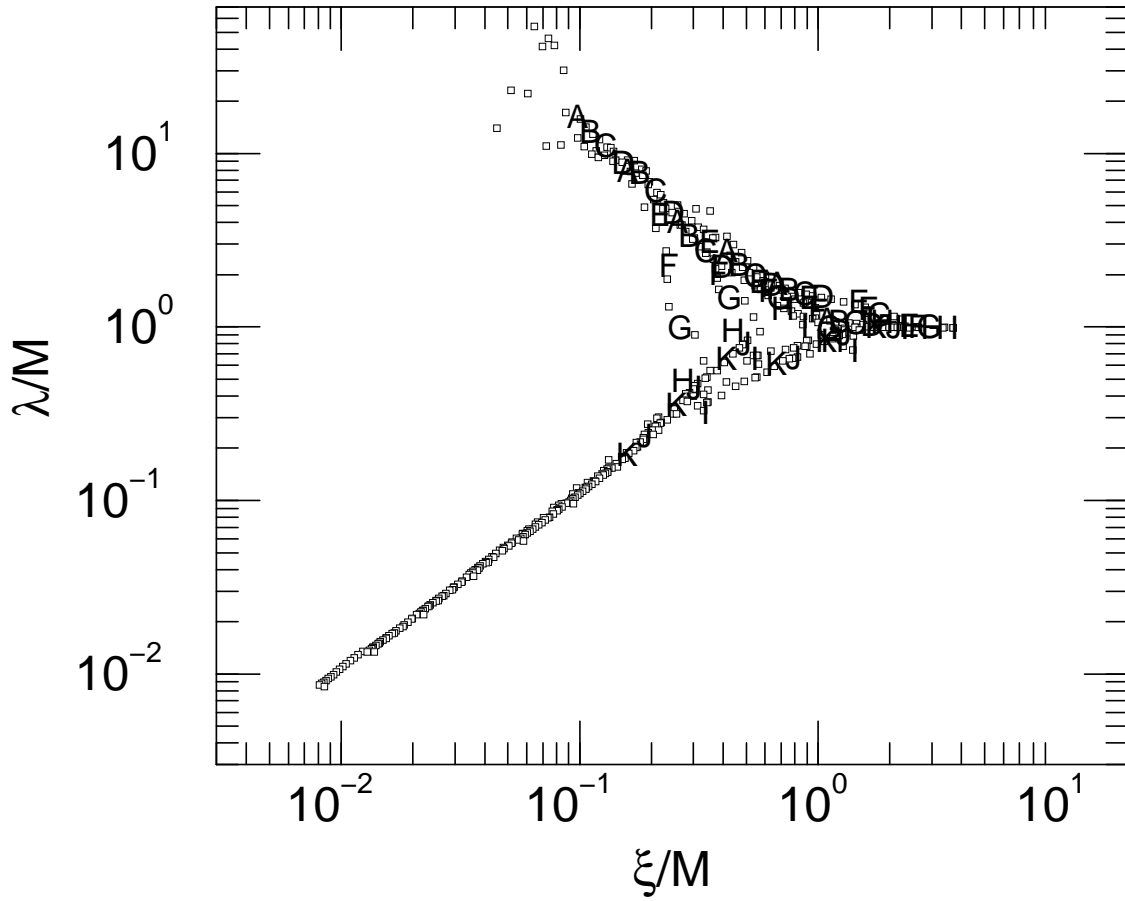


FIG. 5. Scaling function (7) for  $U = 1$ ,  $E = 0$  and various  $\mu$ . The characters are chosen as in Fig. 4.

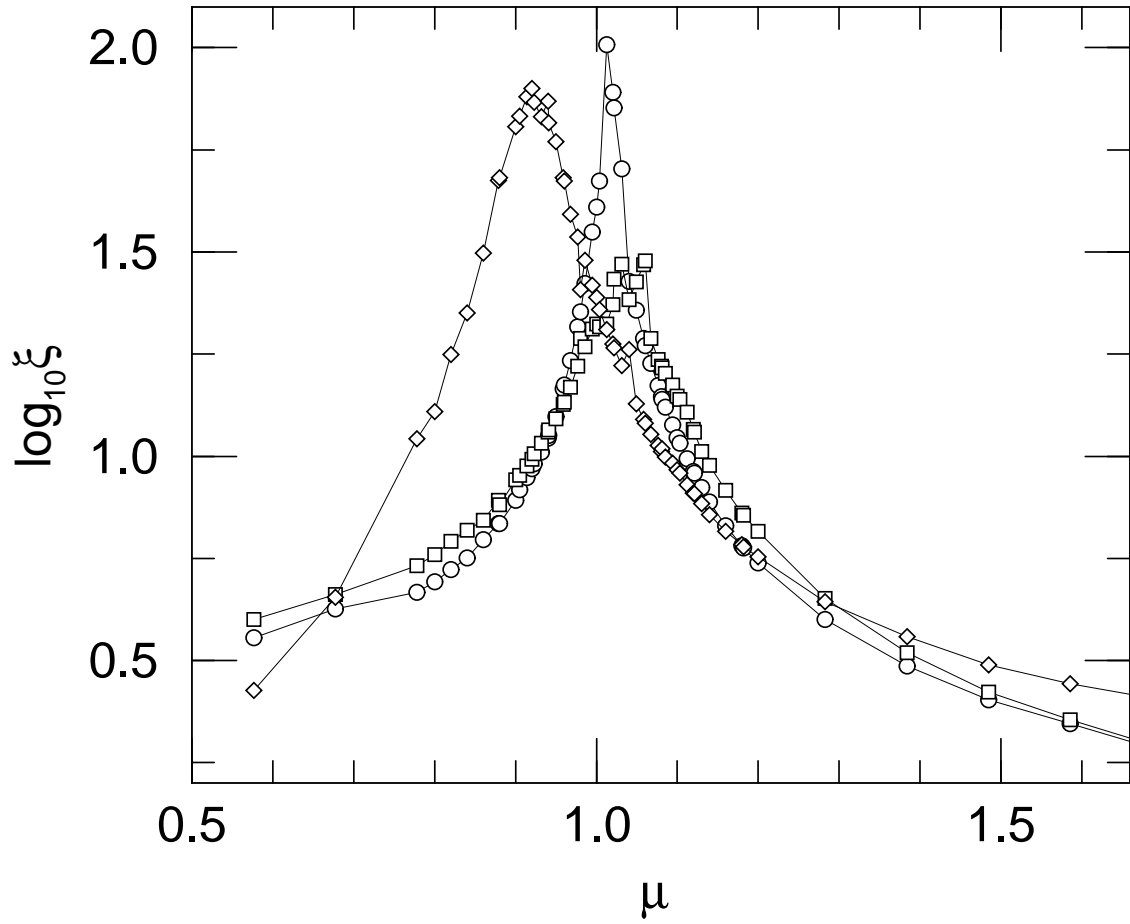


FIG. 6. Scaling parameter  $\xi$  as a function of QP potential strength  $\mu$  for  $U = 0$  ( $\circ$ ), for onsite interaction with  $U = 1$  ( $\square$ ), and for long-range interaction with  $U = 1$  ( $\diamond$ ).

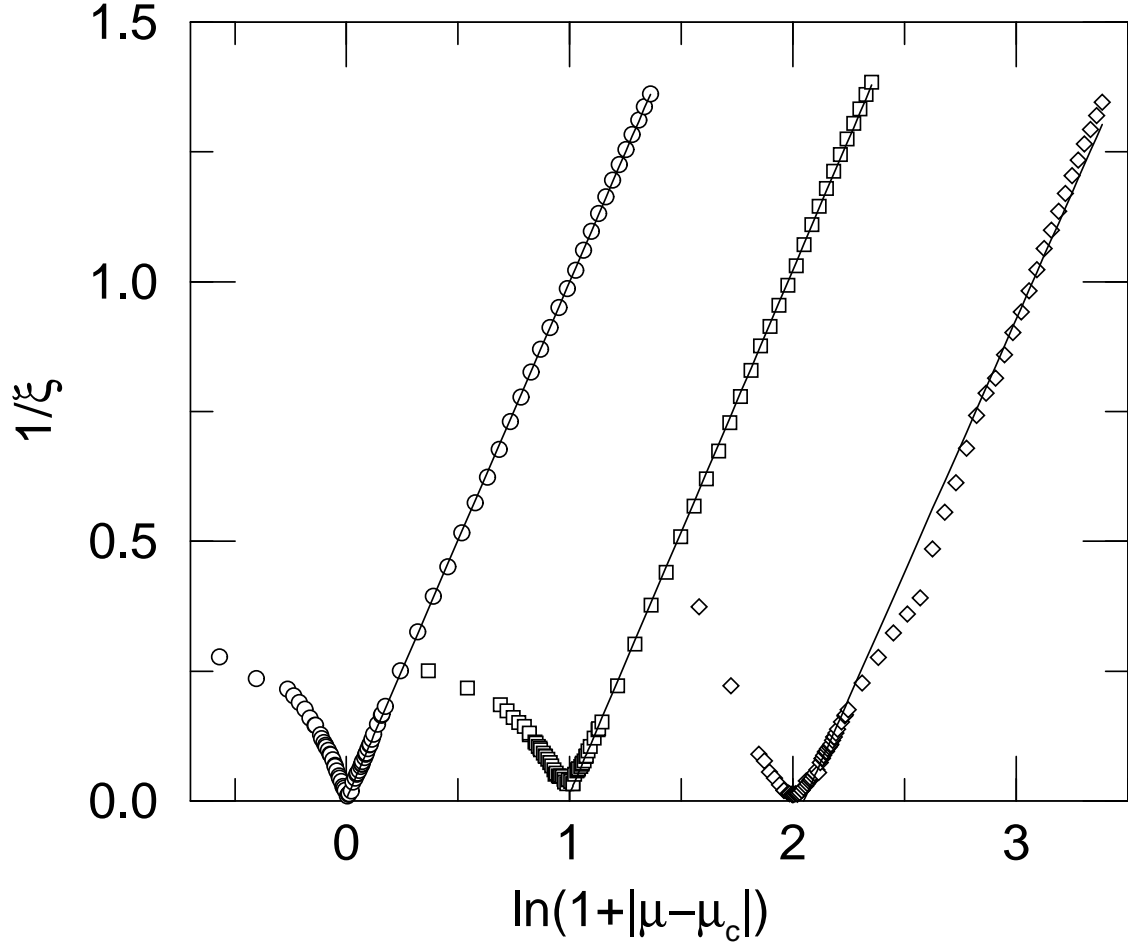


FIG. 7. Inverse scaling parameter  $1/\xi$  as a function of QP potential strength  $\mu$  as in Eq. (8) for  $U = 0$  ( $\circ$ ), for Hubbard interaction with  $U = 1$  ( $\square$ ), and for long-range interaction with  $U = 1$  ( $\diamond$ ), consecutively shifted by 1 for clarity. The lines indicate linear regression fits to the data in the localized regime.





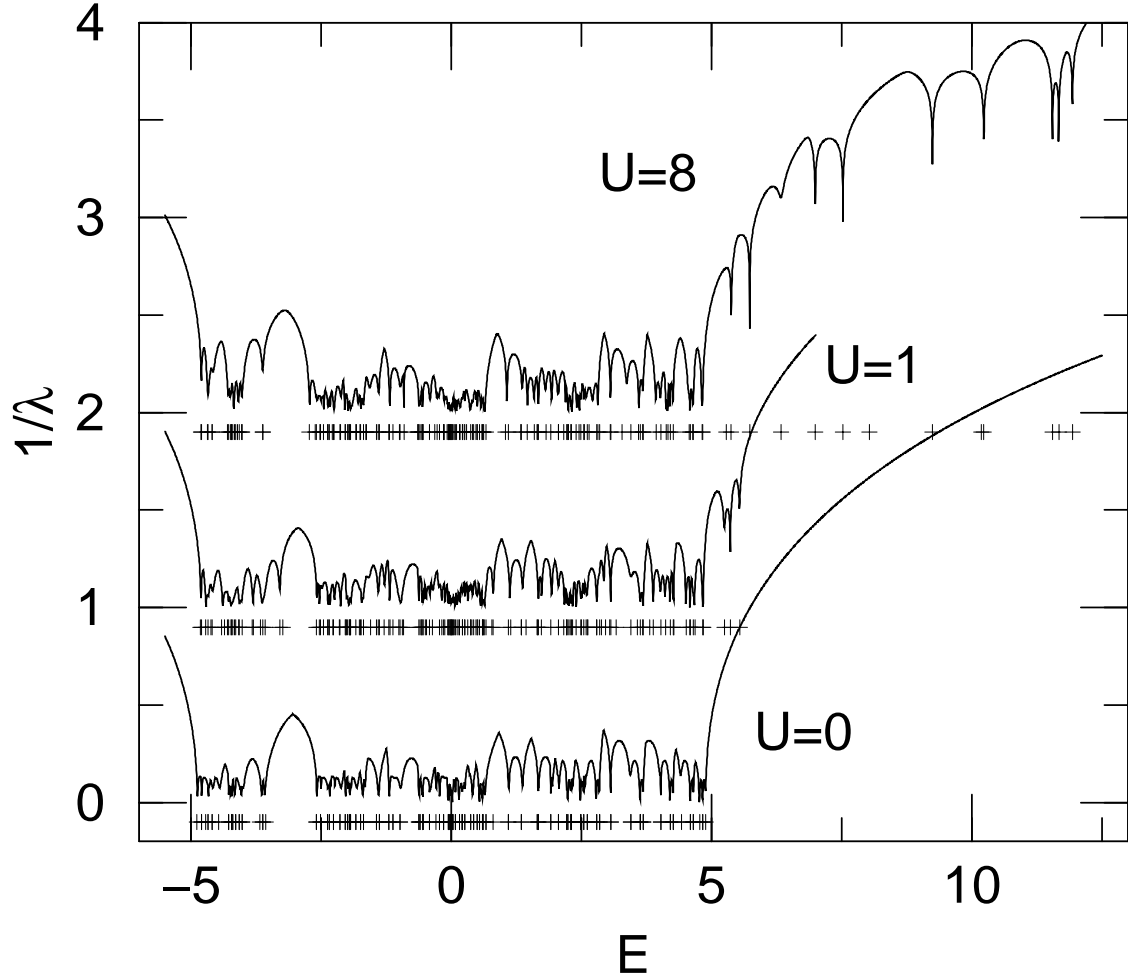


FIG. 9. Inverse localization length as a function of energy for a QP potential strength  $\mu = 0.9$  at  $\beta = \sqrt{2}$ ,  $M = 13$  for  $U = 0$  and for two Hubbard interaction strengths  $U$ . Plots for different  $U$  are vertically shifted for clarity. The eigenenergies are indicated by (+).

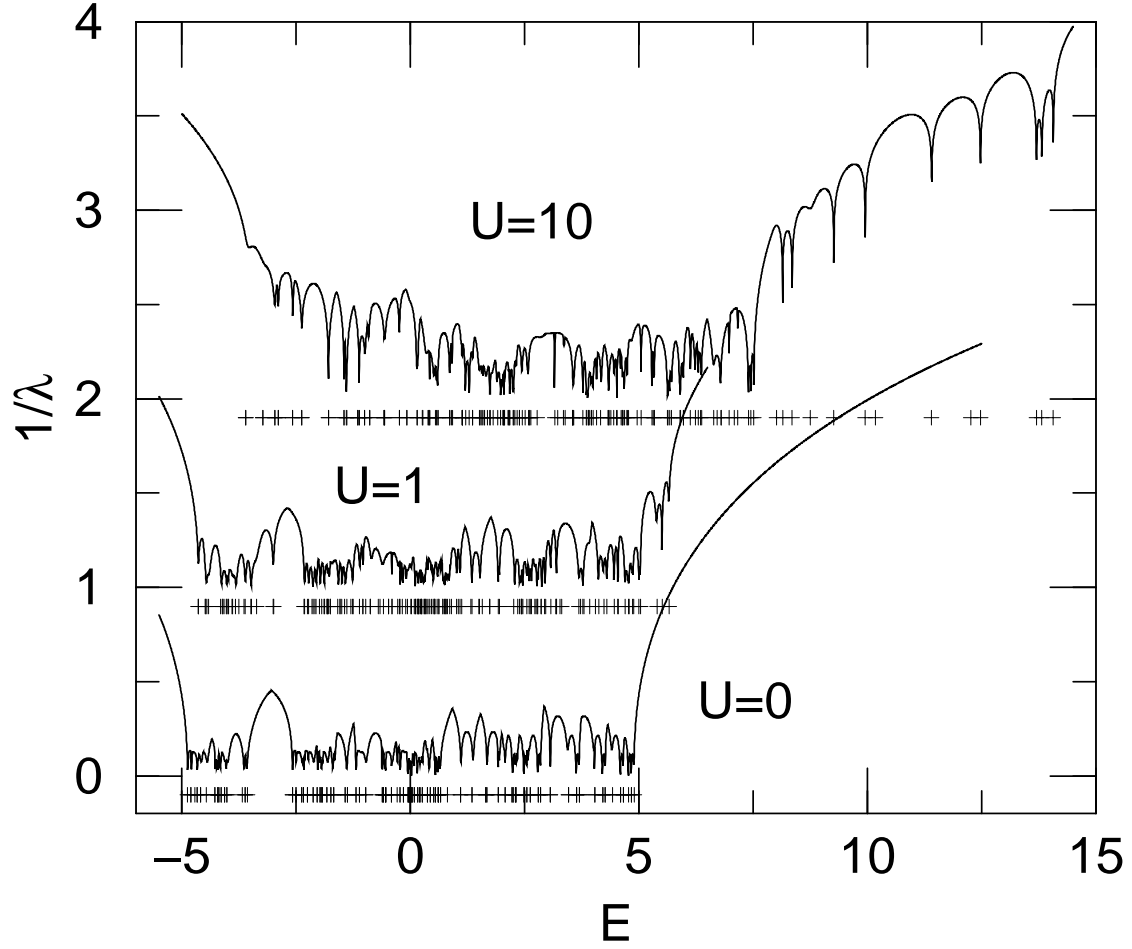


FIG. 10. Inverse localization length as a function of energy for a QP potential strength  $\mu = 0.9$  at  $\beta = \sqrt{2}$ ,  $M = 13$  for  $U = 0$  and two long-range interaction strengths  $U$ . Plots for different  $U$  are vertically shifted for clarity. The eigenenergies are indicated by (+).